Received: 8 February 2021 | Accepted: 16 July 2021 | Published online: 31 August 2021

DOI: 10.1111/opo.12876

OPO THE COLLEGE OF OPTOMETRISTS

ORIGINAL ARTICLE

A validated finite element model to reproduce Helmholtz's theory of accommodation: a powerful tool to investigate presbyopia

Iulen Cabeza-Gil[1] | **Jorge Grasa**[1,2] | **Begoña Calvo**[1,2]

[1]Aragón Institute of Engineering Research (i3A), University of Zaragoza, Zaragoza, Spain

[2]Bioengineering, Biomaterials and Nanomedicine Networking Biomedical Research Centre (CIBER-BBN), Zaragoza, Spain

Correspondence
Iulen Cabeza-Gil, Aragón Institute of Engineering Research (i3A), University of Zaragoza, Zaragoza, Spain.
Email: iulen@unizar.es

Funding information
Ministerio de Ciencia, Innovación y Universidades, Grant/Award Number: DPI2017-84047-R

Abstract

Purpose: To reproduce human in vivo accommodation numerically. For that purpose, a finite element model specific for a 29-year-old subject was designed. Once the proposed numerical model was validated, the decrease in accommodative amplitude with age was simulated according to data available in the literature.

Methods: In contrast with previous studies, the non-accommodated eye condition was the reference configuration. Consequently, two aspects were specifically highlighted: contraction of the ciliary muscle, which was simulated by a continuum electro-mechanical model and incorporation of initial lens capsule stresses, which allowed the lens to become accommodated after releasing the resting zonular tension.

Results: The morphological changes and contraction of the ciliary muscle were calibrated accurately according to the experimental data from the literature. All dynamic optical and biometric lens measurements validated the model. With the proposed numerical model, presbyopia was successfully simulated.

Conclusions: The most widespread theory of accommodation, proposed by Helmholtz, was simulated accurately. Assuming the same initial stresses in the lens capsule over time, stiffening of the lens nucleus is the main cause of presbyopia.

KEYWORDS
accommodative change, finite element method, human eye accommodation, lens shape, presbyopia

INTRODUCTION

Accommodation is a dynamic change in the dioptric power of the eye that allows a change in focus from distant to near objects. This process is achieved by changing the shape of the lens, following contraction of the ciliary muscle, thereby releasing the zonular tension around the lens equator, according to the widely accepted accommodation theory of Helmholtz.[1] Numerous authors have confirmed this theory over time, including Fincham,[2] who demonstrated the ability of the elastic lens to round up after the release of zonular tension, and Glasser and Kaufmann,[3] who showed relaxation of the zonules due to ciliary muscle contraction along with other investigators.[4]

The ciliary muscle is the engine that drives the accommodation process. It consists of three groups of muscle fibres (i.e., longitudinal, radial and circular), although their

division is somewhat arbitrary. There is a gradual transition from the outermost longitudinal muscle fibres through the radial fibres to the innermost circular muscle fibres, with some intermingling of the different fibre types.[4-6] Contraction of the entire ciliary muscle as a whole pulls the anterior choroid forward, moving the apex of the ciliary processes towards the lens equator, and serves the primary function of releasing resting zonular tension at the lens equator to allow accommodation.[4,5] During contraction of the ciliary muscle, the circular portion of the ciliary muscle tends to increase in thickness, whilst the radial and longitudinal portions decrease in thickness.

The crystalline lens is the ocular element that alters the focal length of the eye. During accommodation, the human lens undergoes several changes: its diameter decreases, its thickness increases, the anterior and posterior surfaces of the lens move anteriorly and posteriorly, respectively and the curvatures of the anterior and posterior surfaces of the lens increase. Moreover, the thickness of the lens nucleus increases, but without a significant change in thickness of the cortex.[4,7] Several authors have designed finite element (FE) models to explain and understand accommodation.[8-15] However, most of these biomechanical models are based on accommodated geometry, and reproduced the accommodation process in reverse by applying the forces exerted by the relaxation of the ciliary muscle to reach the non-accommodated state. These FE models are a powerful tool to understand the opto-mechanical crystalline lens changes. However, *in vivo* accommodation cannot be reproduced faithfully through these tests, and thus some key aspects of accommodation which involves other tissues (ciliary muscle, sclera) cannot be analysed properly. In contrast to these previous studies, the reference configuration of our FE model is the non-accommodated state, which is the resting state of the physiological system.

We propose a 3-dimensional FE model that incorporates contraction of the ciliary muscle to reproduce *in vivo* human accommodation. This FE model is standardised for a 29-year-old subject as there is sufficient comparative and physiological data in the literature to develop the model and evaluate it with experimental data. Ciliary muscle contraction is simulated with an electro-chemical-mechanical continuum model.[16,17] Moreover, to allow the lens to change its shape after release of zonular tension, the initial stresses of the lens capsule are included in the model.

The proposed FE model was validated by comparison with the experimental optical and main biometric changes during human *in vivo* accommodation provided by Ramasubramanian and Glasser.[18,19] To achieve this aim, the ciliary muscle contraction was calibrated by comparing the morphological changes with the recent work of Wagner *et al*.,[20] who evaluated ciliary muscle thickness (CMT) profiles derived from optical coherence tomography (OCT) images during *in vivo* human accommodation.

With the proposed FE model, the physiological decrease in accommodation amplitude with age was evaluated and compared with experimental data.[21-23] A sensitivity analysis of the mechanical properties of the crystalline lens as a function of age was performed to observe the most influential mechanical factors in the development of presbyopia.[24-26]

Key Points

- A novel finite element model that reproduces ocular accommodation is presented. The decrease in accommodative amplitude with age was reproduced using the proposed model.
- The main cause of presbyopia is the stiffening of the lens nucleus with age.
- The numerical model can help to understand human accommodation.

Justification of the geometry and the 3-dimensional FE model are presented in the Method section, followed by a description of the constitutive laws of all materials involved, including the formulation of the active behaviour of the ciliary muscle and the mechanical properties used to analyse the decrease in accommodation amplitude with age. Methodology is provided to analyse the optical and biometric changes during accommodation. The results of these changes are presented together with some calibration parameters of the muscle activation. Once the ciliary muscle is engaged, it is coupled with the accommodation system to simulate the change in shape of the lens, and thus the refractive power change. An analysis of the decrease in accommodation amplitude with age is shown.

MATERIALS & METHODS

Finite element model

To obtain the most realistic representation possible, this model of the accommodation system comprises the most relevant components in the accommodation process: the shell of the eye composed of the cornea and sclera; iris; lens nucleus, cortex and capsule; zonules of Zinn divided into anterior and equatorial zonules and the ciliary body, which is composed of the ciliary muscle and processes.

Figure 1 shows the dimensions of the different components of the FE model in the non-accommodated state standardised for a 29-year-old subject. Lens dimensions were obtained from the OCT study of Chang *et al*.,[27] with a radius of curvature of the anterior (r_a) and posterior (r_p) lens surfaces of 11.00 and 6.10 mm, respectively, sagittal thickness of the lens (T_L) of 3.44 mm and an anterior chamber depth (*ACD*) of 3.03 mm. As the lens equatorial diameter cannot be obtained by OCT, it was extracted from the MRI work of Kasthurirangan *et al*.[29] with the value of 9.04 mm being obtained. The anterior and posterior thickness of the lens cortex were 0.80 mm and 0.50 mm, respectively, with

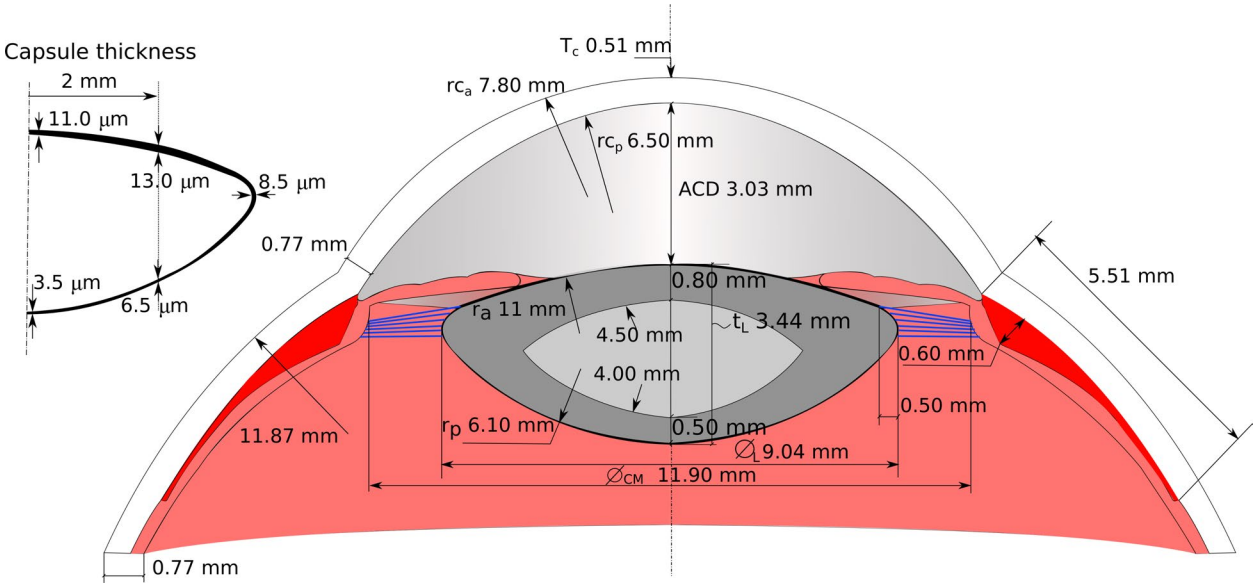

FIGURE 1 Dimensions of the finite element (FE) model. It includes the lens, the zonules of Zinn (blue), the ciliary muscle (red), the iris and ciliary processes (light pink) as well as the sclera and cornea (white). A detailed view reflecting capsule thickness is shown on the left. Due to the lack of available data in the literature, the thickness distribution of the lens capsule used was taken from a 36-year-old subject[28]

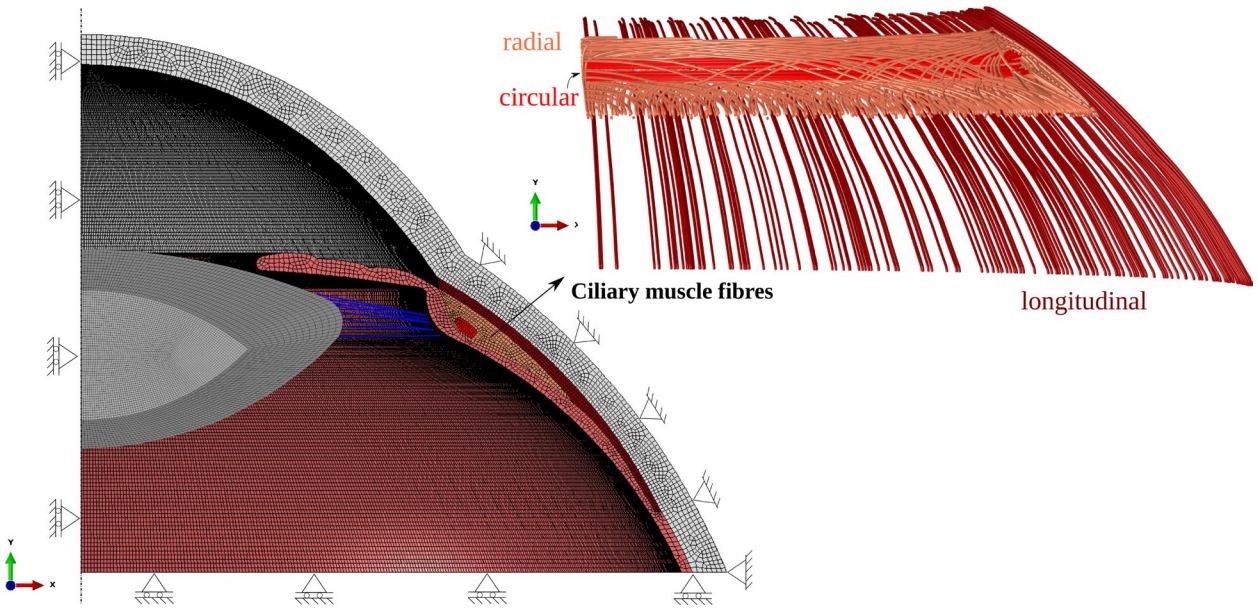

FIGURE 2 3D finite element (FE) model of the accommodative system: lens, zonules, ciliary muscle, iris, sclera and cornea. The arrangement and orientation of the ciliary muscle fibres, longitudinal (yellow), radial (orange) and circumferential (red), is shown on the right. The FE model contained 402,373 elements

an anterior and posterior surface radius of curvature of 4.50 and 4.00 mm, respectively.[30,31] Zonules were anchored 0.50 mm in the anterior capsule based on Bernal *et al.*,[32] and the ciliary body ring diameter was 11.90 mm.

The averaged ciliary muscle geometry of emmetropic eyes reported by Wagner *et al.*[20] was used in our model. In their study, the geometry was provided by a CMT profile, which was obtained from OCT images following the methodology of Straßer *et al.*[33] Therefore, an in-house code in MATLAB 2020b (MathWorks, mathworks.com) with the inverse methodology[33] was created and implemented to obtain the geometry from the CMT profile.

The ciliary muscle was arranged into three families of muscle fibres, i.e., circular, radial and longitudinal, according to the distribution reported by Pardue and Sivak.[6] The volume percentage of the circular, radial and longitudinal muscle fibres is 12%, 33% and 55% respectively, and their distribution is shown in *Figure 2*.

Considering that the material model allows only one preferential direction, the orientation of the radial fibres was defined as a transition from the circular to the longitudinal fibres; see *Figure 2*.

Regarding the iris, a trabecular-iris angle of 40° and a thickness at 750 μm from the scleral spur of 0.40 mm were considered for visual effects since its contraction was not considered.[34,35] Finally, the shell of the eye was designed according to the Le Grand[36] model. The thickness of the sclera and cornea were readjusted for a 29 year old subject[37]; see *Figure 1*.

Considering all the above-mentioned factors regarding the geometry, a 3-dimensional FE mesh of the anterior half of the ocular globe was designed. Due to the symmetry, only a quarter of the geometry was considered, ensuring the corresponding symmetry boundary conditions. Axial displacements were restrained at the bottom scleral surface. Moreover, the exterior surfaces of the sclera were fixed by the extraocular muscles. The general-purpose finite element code Abaqus FEA version 14.1 (Simulia, 3ds.com) was used to build the FE model. A mesh sensitivity analysis was performed in order to establish the final mesh size; see *Figure 2*. The lens nucleus and cortex were considered solid bodies and were meshed with 96,640 hybrid linear hexahedral (C3D8H) elements; the capsule was meshed with 5290 4-node membrane (M4) elements; 546 zonules were modelled using Abaqus connector elements, whose nonlinear behaviour is explained below; the ciliary muscle was meshed with 94,809 linear hexahedral (C3D8) elements and the ciliary body was meshed with 201,110 C3D8 elements and 3978 linear wedge (C3D6) elements.

The fluids filling the eye, namely the aqueous and vitreous humours, were not included in the model as we considered that there is a homogeneous pressure inside the eye during accommodation. Due to the boundary conditions applied in the sclera, the eyeball structure is stable.

Material behaviour

Ciliary muscle

The process of smooth muscle contraction can be initiated by mechanical, electrical or chemical stimuli. The contractile mechanism involves several signal transduction pathways, all of which converge to increase the intracellular calcium concentration, resulting in phosphorylation of myosin.[38] Regarding the ciliary muscle, the action of the neurotransmitter acetylcholine on post-synaptic muscarinic receptors controls muscle activation. This system forms part of the parasympathetic branch of the autonomic nervous system. On the other hand, an inhibitory effect is driven by the sympathetic system, which is mediated principally by the action of the neurotransmitter noradrenaline on β_2 receptors.[39]

In this work, the passive and active finite strain response of the ciliary muscle was simulated within the framework of continuum mechanics using a common methodology based on postulating the existence of a strain energy density function (SEF).[16,17] This function depends on a series of state variables related to the deformation of the active and passive elements, the contraction level and the muscle fibre arrangement:

$$\Psi = \Psi(\mathbf{C}, \mathbf{C}_e, \lambda_a, \mathbf{N}). \tag{1}$$

$\mathbf{C} = \mathbf{F}^T\mathbf{F}$ is the right Cauchy–Green deformation tensor with $\mathbf{F}$ the deformation gradient. $\mathbf{C}_e$ is an equivalent deformation tensor associated with the deformation of the elastic components in the muscle, and it arises from a two-step formulation of the contraction process.[16] From this formulation, a decomposition of the strain deformation gradient is proposed as $\mathbf{F} = \mathbf{F}_e\mathbf{F}_a$. Therefore, the elastic deformation gradient can be defined as $\mathbf{C}_e = \mathbf{F}_e^T\mathbf{F}_e$. λ_a is the contraction or stretch of the active component of the muscle fibres that forms the active strain deformation gradient $\mathbf{F}_a$ assuming

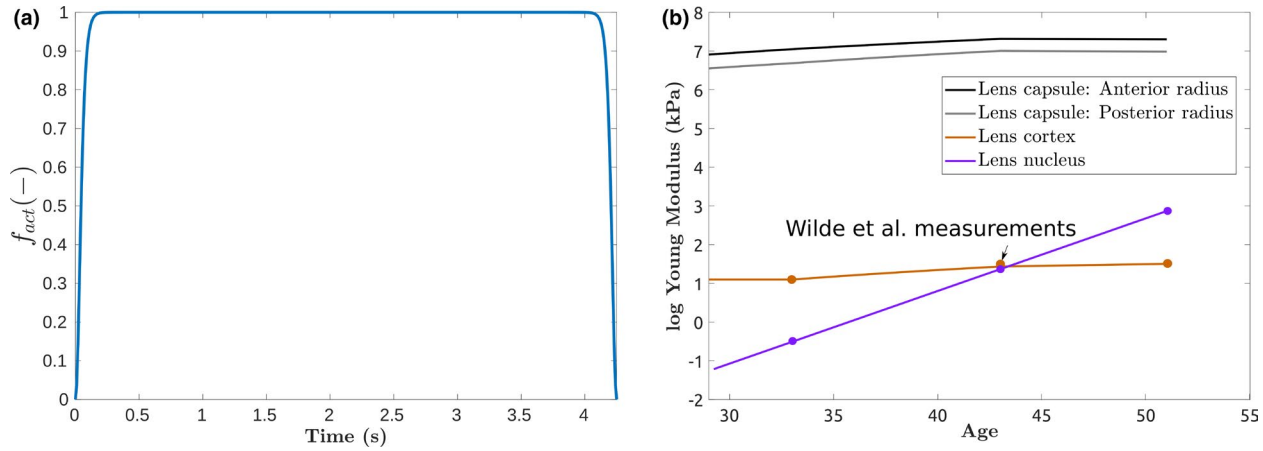

FIGURE 3 (a) Activation function of the ciliary muscle and (b) mechanical properties of the crystalline lens used in this study. There is a circle in the lens nucleus and cortex plot indicating the values reported by Wilde *et al.*[26] The mechanical properties of the lens capsule were characterised by Krag and Andreassen[41,42]

incompressibility.[16] The structural tensor $\mathbf{N} = \mathbf{n}_0 \otimes \mathbf{n}_0$ defines the anisotropy of the muscle due to the direction of muscular fibres $\mathbf{n}_0$.

The SEF is decoupled into volume-changing and volume-preserving parts in order to handle the quasi-incompressibility constraint. Furthermore, the deviatoric part is divided into a passive contribution due to the collagen and elastin, $\overline{\Psi}_p$, and an active contribution associated with the muscular fibres, $\overline{\Psi}_a$. Thus, the total strain energy function Ψ can be expressed as follows:

$$\Psi = \Psi_{vol}(J) + \overline{\Psi}_p(\overline{\mathbf{C}}, \mathbf{N}) + \overline{\Psi}_a(\overline{\mathbf{C}}_e, \overline{\lambda}_a, \mathbf{N}), \tag{2}$$

where the relations $\overline{\mathbf{C}} = J^{-2/3}\mathbf{C}$, $\overline{\mathbf{C}}_e = J^{-2/3}\mathbf{C}_e$ and $\overline{\lambda}_a = J^{-1/3}\lambda_a$ have been applied with $J = det(\mathbf{F})$ being the Jacobian of the transformation. Equation 2 can be particularised for the behaviour of the ciliary muscle and formulated in a more proper way for computational purposes as:

$$\Psi = \Psi_{vol}(J) + \overline{\Psi}_p(\bar{I}_1, \bar{I}_2, \bar{I}_4) + f_\lambda f_{act}\overline{\Psi}'_a(\bar{J}_4). \tag{3}$$

where f_λ is the force-stretch relationship that account for the actin and myosin overlap, f_{act} is the activation function and $\overline{\Psi}_a$ is the active SEF. The passive SEF, $\overline{\Psi}_p$, is defined as a function of the invariants of the isochoric right Cauchy-Green tensor:

$$\bar{I}_1 = tr\overline{\mathbf{C}}, \qquad \bar{I}_2 = \frac{1}{2}((tr\overline{\mathbf{C}})^2 - tr\overline{\mathbf{C}}^2), \qquad \bar{I}_4 = \mathbf{n}_0.\overline{\mathbf{C}}\mathbf{n}_0 = \overline{\lambda}^2, \tag{4}$$

where $\bar{I}_1$ and $\bar{I}_2$ are the first and second modified strain invariants and $\bar{I}_4$ is the invariant related to the anisotropy of the passive response. According to the SEF proposed by Calvo *et al.*,[40] the passive response $\overline{\Psi}_p$ can be written:

$$\overline{\Psi}_p = c_1(\bar{I}_1 - 3) + \frac{c_3}{c_4}(e^{c_4(\bar{I}_4 - \bar{I}_{4_0})} - c_4(\bar{I}_4 - \bar{I}_{4_0}) - 1). \tag{5}$$

The active SEF, $\overline{\Psi}_a$, associated with the active response, and consequently with the actin-myosin interaction, is expressed as the product of two functions that scale the energy stored due to contraction in the elastic element $\overline{\Psi}'_a$.[16] The influence of filament overlap on the active response of the muscle f_λ is formulated in terms of the muscle fibre stretch $\overline{\lambda}_a$, the optimum stretch λ_{opt} and the coefficient ξ:

$$f_\lambda = e^{\frac{-(\bar{\lambda}_a - \lambda_{opt})^2}{2\xi^2}}. \tag{6}$$

The activation function f_{act} is assumed to represent the excitation input signal that triggers the contraction independently of its origin. In this work, the product of two squared hyperbolic tangents has been selected as:

$$f_{act} = (\tanh^2(s_1(t - t_i))\tanh^2(s_2(t - (t_i + t_s))), \tag{7}$$

where s_1 and s_2 regulate the initial and final slope of the function, respectively, t is the time variable, and t_i and t_s define the start of the activation and the stimulus duration, respectively. *Figure 3a* shows the activation function used in the study. The energy stored in the cross-bridges is expressed in terms of the invariant associated to $\overline{\mathbf{C}}_e$ in the direction of the muscle fibres $\mathbf{n}_0$:

$$\overline{\Psi}'_a = \frac{1}{2}P_0(\bar{J}_4 - 1)^2, \bar{J}_4 = \mathbf{n}_0.\overline{\mathbf{C}}_e\mathbf{n}_0 = \overline{\lambda}_e^2. \tag{8}$$

where P_0 is a proportionality factor related to the maximum active stress due to muscle contraction.[16]

Due to the non-recoverable deformation that occurs in the active part of the muscle fibres (its initial shape is only recovered with the help of the elastic components), the model incorporates a dissipation energy rate associated with active stresses and strains.[16] Using the second law of thermodynamics in the shape of the Clausius-Planck inequality and neglecting the thermal dissipation rate, some of the power produced internally is stored while another portion is dissipated.[16] From this expression, two constitutive relationships can be derived. The first one is used to obtain the classical relation between the derivative of the so-called strain energy density function with respect to the elastic strain tensor and the second the Piola-Kirchhoff stress tensor. The second relationship allows establishment of the evolution of the contraction velocity $\dot{\overline{\lambda}}_a$ as a function of the same strain energy and stresses[16]:

$$P_a - \frac{\partial\overline{\Psi}}{\partial\overline{\lambda}_a} + \left(2\overline{\mathbf{C}}_e\frac{\partial\overline{\Psi}}{\partial\overline{\mathbf{C}}_e}\overline{\mathbf{F}}_a^{-T}\right) : \frac{\partial\overline{\mathbf{F}}_a}{\partial\overline{\lambda}_a} = C\dot{\overline{\lambda}}_a, \tag{9}$$

where $P_a = -\tilde{v}P_0f_\lambda f_{act}$ is the active stress, with $\tilde{v}$ being a friction parameter that considers the relative sliding speed between actin and myosin. The parameter C is defined as:

$$C = \frac{1}{v_0}P_0f_\lambda f_{act}, \tag{10}$$

where v_0 is associated with the initial contraction velocity. A set of preliminary analyses, explained in the Results section, was performed to obtain the parameters P_0 and v_0 of the active behaviour of the ciliary muscle; see *Tables 1* and *2*.

Constitutive laws of the remaining tissues

The whole lens was modelled with an elastic behaviour. The lens capsule was modelled via membrane elements, assuming pure traction behaviour. In turn, the lens capsule was divided into anterior and posterior regions, characterising their mechanical properties differently based on the work of Krag and Andreassen,[41,42] see *Table 3*.

In contrast with those of the lens capsule, the mechanical properties of the lens nucleus and cortex are unclear and somewhat controversial. Burd *et al.*[43] reported that Fisher's[24] spinning lens measurements might not be

TABLE 1 Parameters of the active behaviour of the continuum model adapted for the smooth ciliary muscle

Active behaviour								
λ_{opt} (–)	ξ(–)	t_s	t_i	s_q	s_2	P_0(*MPa*)	v_0(–)	$\tilde{v}$(–)
1.00	0.16	4.25	0.00	20.00	20.00	1.50	0.90	0.59

TABLE 2 Parameters of the passive behaviour of the ciliary muscle

Passive behaviour			
c_1(*kPa*)	c_3(*kPa*)	c_4(–)	$I4_0$ (–)
8.37	9.87	2.23	1.25

TABLE 3 Mechanical properties of the different tissues of the FE model for the subject of 29 years old

	E (*kPa*)	ν (–)	C_1 (*kPa*)	D_1 (kPa^{-1})	References
Nucleus	0.30	0.49	–	–	25,26
Cortex	3.00	0.49	–	–	25,26
Anterior capsule	1000	0.49	–	–	41,42
Posterior capsule	700	0.49	–	–	41,42
Sclera	–	–	102.73	89.71	46
Cornea	–	–	222.64	194.13	47
Ciliary processes	–	–	0.80	0.70	48

Note: The lens was modelled through an elastic behaviour (Young modulus), whilst the remaining parts of the accommodative system were modelled with a neo-Hookean hyperelastic model.

reliable, and relatively few subsequent studies regarding the mechanical properties of the internal lens have been performed,[25,26,44] with slight differences being observed between them. We determined the values reported by Wilde *et al.*,[26] taking into account the stress–strain relationship E = 3G, with G being the shear modulus, can be considered for isotropic elastic linear and incompressible materials. Due to the lack of data, we extrapolated values from a 33-years-old lens to a 29-years-old one; see *Figure 3b*.

The cornea, sclera and ciliary processes were modelled through an isotropic, quasi-incompressible Neo-Hookean hyperelastic model. The material properties for the 29-year-old subject were chosen from the data available in the literature, as displayed in *Table 3*.

The zonules were modelled with linear connector elements as Helmholtz's accommodation theory postulates,[1,2] i.e., they are stretched in the non-accommodated state, which is the reference configuration. This was considered as an initial force value F_0 in the force-displacement equation that defines their behaviour:

$$F(u) = F_0 + ku, \tag{11}$$

with F_0 = 50 mN, k = 100 mN mm^{-1} and u being the displacement in the direction of the zonule (element).[45] No compression was considered.

Analysis procedure

The most common theory of accommodation, proposed by Helmholtz,[1] was considered, and the contraction and relaxation of the ciliary muscle were reproduced in order to simulate the distant (non-accommodated) and near vision (accommodated) states.

The reference configuration of the FE model corresponds to the non-accommodated geometry, where the lens capsule and the Zinn zonules are not stress free. The decapsulated lens substance assumes a maximally unaccommodated form after removing the capsule, and thus the decapsulated lens was initially stress free.[49] The initial stress distribution (σ_{ij}^0) was obtained with an extra analysis, stretching the lens from the accommodated to the non-accommodated state; see Figure 4a. The stress results at the integration points were mapped to the new lens capsule geometry.

All dynamic optical and biometric lens measurements of the accommodation mechanism were evaluated for each increment of the evolution process modelled in the simulation. For that purpose, displacement of the lens nodes and nucleus contour were registered by an URDFIL Abaqus subroutine and post-processed with MATLAB R2020b.

To measure the actual accommodative change (difference between the non-accommodated and corresponding accommodated states), the central optical power of the eye (COP_{Eye}) was evaluated throughout the simulation using Gullstrand's eye formula:

$$\mathrm{COP}_{Eye} = COP_c + COP_L - \frac{ACD}{n_a} COP_c COP_L, \tag{12}$$

with the central optical powers of the lens (COP_L) and the cornea (COP_C)[8]:

$$COP_L = \frac{n_L - n_a}{r_a} + \frac{n_L - n_a}{r_p} - \frac{T_L (n_L - n_a)^2}{r_p r_a n_L}, \tag{13}$$

$$COP_C = \frac{n_c - n_{air}}{rc_a} + \frac{n_a - n_c}{rc_p} - \frac{(n_c - n_{air})(n_a - n_c) T_c}{n_c rc_a rc_p}, \tag{14}$$

where n_a = 1.336 is the refractive index of the aqueous humour, n_L = 1.42 is the estimated overall refractive index of the lens, n_c = 1.376 is the refractive index of the cornea and n_{air} = 1.00 is the refractive index of air. The remaining biometric terms, r_a, r_p, T_L, *ACD*, rc_a, rc_p and T_c, defined in *Figure 1*, vary throughout the simulation. The power of the cornea was

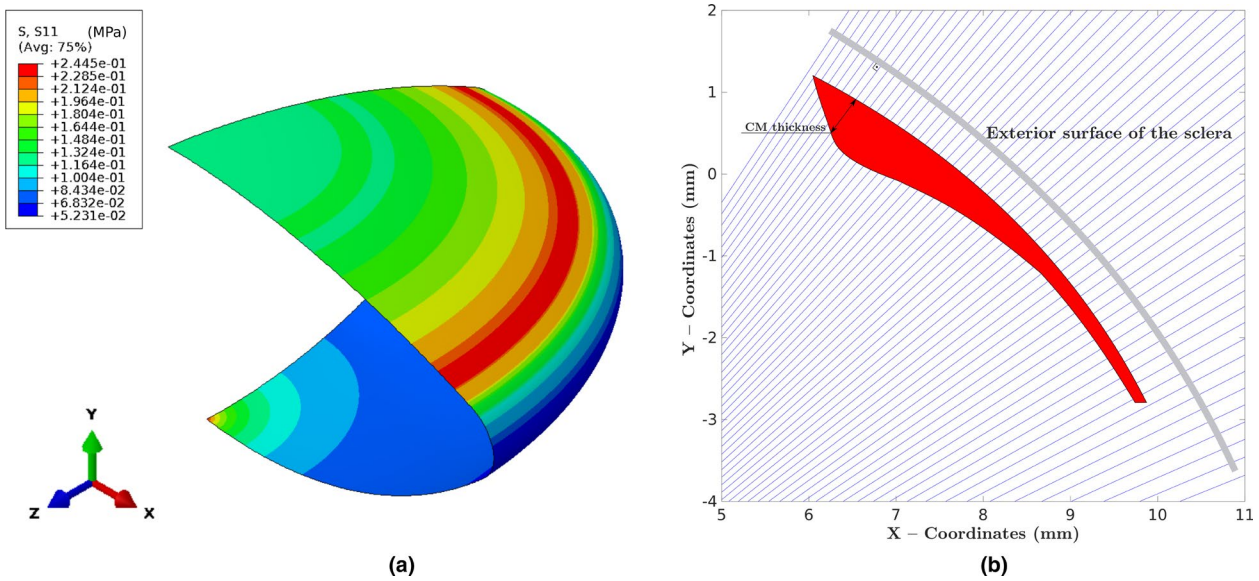

FIGURE 4 (a) Stress distribution (σ_x^0) of the lens capsule in the non-accommodated state. This stress distribution makes the lens accommodate after the zonular tension is released. $\sigma_x^0 \approx \sigma_y^0$, with $\sigma_z^0 = 0$ due to the state of plane stress considered. (b) optical coherence tomography (OCT) measurement technique used to evaluate ciliary muscle thickness (CMT) profiles during accommodation[33]

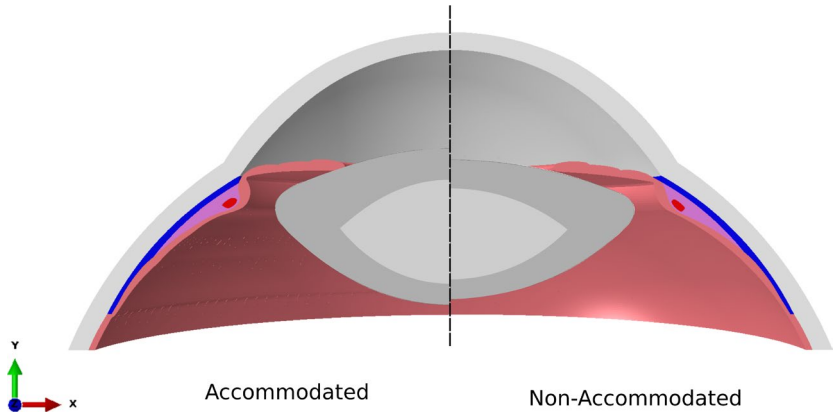

FIGURE 5 Numerical solution of the accommodated state (left) and non-accommodated state (right). The accommodated state and the reference configuration provide 63.82 D and 58.00 D, respectively

kept constant throughout the simulation. The radii of curvature were calculated throughout the stretching process through an equation for a conic section having an apex at the origin and tangent to the y axis.

$$y^2 - 2rx + (K+1)x^2 = 0. \tag{15}$$

To obtain the corresponding radius of curvature (r) and the conic constant (K), a non-linear system of equations formed by the coordinates of the nodes (x, y) was solved. The goodness of the fit was $R^2 > 99\%$. The standardised design of the eye had 58 dioptres (D) in the far-vision state.

Lastly, the deformed geometry of the ciliary muscle was also measured during accommodation for each increment of the evolution process modelled in the simulation. Straßer's[33] methodology was used to measure the CMT profile along the overall length of the muscle, which consists of measuring the distance between the sclera and the outer boundary of the ciliary muscle from perpendicular rays originating in the exterior surface of the sclera; see *Figure 4b*.

RESULTS

During ciliary body contraction, the zonules release tension to allow the lens to round up to its accommodated state, see *Figure 5*. The FE solution, corresponding to an actual accommodation amplitude of 5.82 D, is shown on the left whilst the reference configuration, the non-accommodated state is depicted on the right to show

the geometrical changes, mainly in the ciliary muscle and lens.

To evaluate the accuracy of the proposed FE model of accommodation, we compared the dynamic changes produced in the ciliary muscle and lens during accommodation with experimental values collected from the literature.

Ciliary muscle contraction

Figure 6 shows the morphological comparison between the numerical and experimental ciliary muscle contraction.[20] The experimental ciliary muscle contraction corresponds to an accommodation stimulus of 4 D.[20] The actual accommodative response is lower than the accommodation stimulus.[50,51] *Figure 6a* presents the contour of both the non-deformed and deformed geometries, while *Figure 6b* depicts comparison between the numerical and experimental CMT profiles.[20]

Once the numerical and experimental contractions of the ciliary muscle were compared, we calibrated the main parameters of active behaviour of the ciliary muscle, maximum active stress (P_0) and the initial contraction velocity (v_0) in order to reproduce the contraction and relaxation of the ciliary muscle. The maximum active stress is related to the maximum change in the ciliary muscle ring diameter (ϕ_{CM}), whereas the initial contraction velocity (v_0) is related to the temporal performance of the muscle contraction. Due to the lack of data in the literature, we calibrated the muscle properties based on a virtual case.[52] Glasser *et al*.[52] provided electrical innervation to quantify the changes in lens diameter in rhesus monkeys. The virtual case attempted to replicate this situation but by quantifying the change in the ciliary body ring diameter. An accommodation square wave was implemented for 4 s by simulating electrical innervation. For the maximum electrical innervation, a maximum change in $\Delta\phi_{CM}$ of 0.70 mm was presumably obtained. The methodology proposed would be the same for an actual case.

These properties were calibrated by means of a sensitivity analysis observing $\Delta\phi_{CM}$. First, the maximum active stress (P_0) was obtained at the maximum response amplitude, 0.70 mm.[52] To do so, P_0 ranged from 0.50 to 2.00 MPa, with $v_0 = 3.00$ based on a previous study.[17] *Figure 7a* shows that a $\Delta\phi_{CM}$ of 0.70 mm is obtained for $P_0 = 1.50$ MPa. Once the maximum active stress was achieved, sensitivity analysis of the initial contraction velocity, v_0, was performed to calibrate the temporal performance (activation and deactivation) of the ciliary muscle; see *Figure 7b*.

Coupling of the ciliary muscle and lens

Before analysing the dynamic biometric and optical measurements of the lens, we will describe the joint performance of the ciliary muscle and lens. *Figure 8* presents three conditions of the ciliary muscle and lens based upon different accommodated states, namely, at 0.00, 0.75 and 1.50 s, which correspond to different ciliary body ring diameters ($\Delta\phi_{CM}$). The numerical FE model presented a maximum accommodation of 5.82 D.

The accommodative response followed a linear relationship with the $\Delta\phi_{CM}$, with an increase of 5.82 D and an increase in lens thickness of 0.44 mm for a reduction of 0.66 mm in $\Delta\phi_{CM}$ or 67.54 μm in ΔCMT_{max}. Due to the way in which the CMT profiles are obtained with the perpendicular rays from the sclera, the changes observed in the CMT profiles are of lower magnitude.

Dynamic optical and biometric lens measurements

The experimental *in vivo* results in humans obtained by Ramasubramanian and Glasser[18,19] were used for comparison with the numerical dynamic optical and biometric lens measurements. *Figure 9a* shows the changes in the anterior

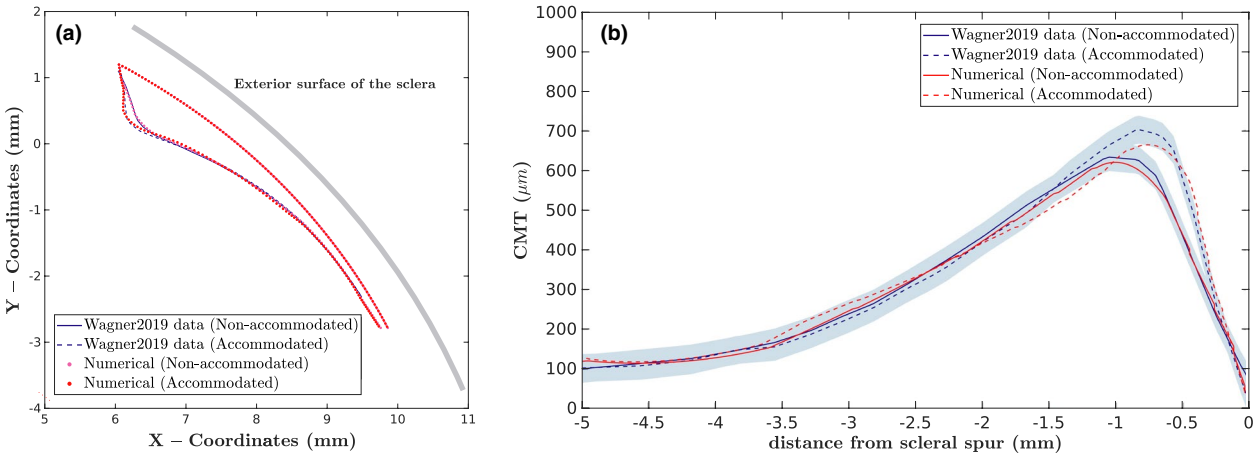

FIGURE 6 Comparison between the morphological changes in ciliary muscle contraction. (a) In blue: the experimental ciliary muscle contour before and after contraction; in red: the numerical result. (b) Comparison between the experimental and numerical CMT profiles during far and near (4D) accommodation

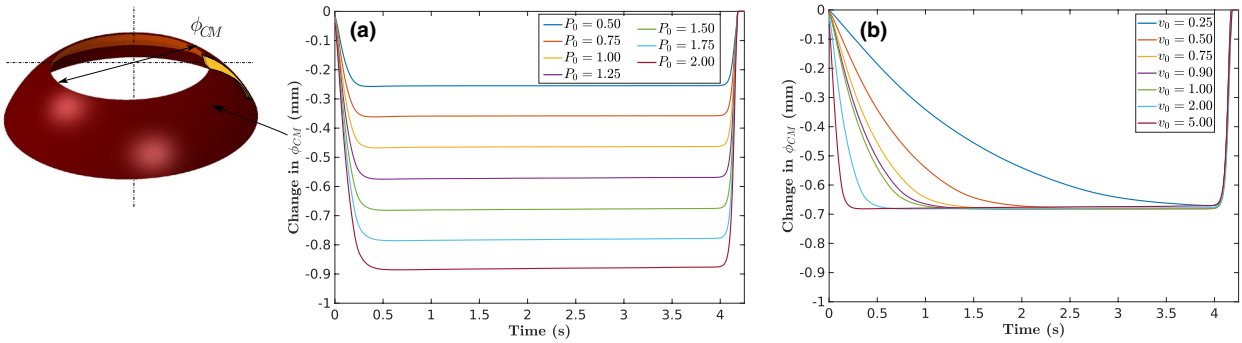

FIGURE 7 Calibration of the ciliary muscle properties by means of a sensitivity analysis of: (a) the maximum active isometric stress (P_0) and (b) the initial velocity (v_0)

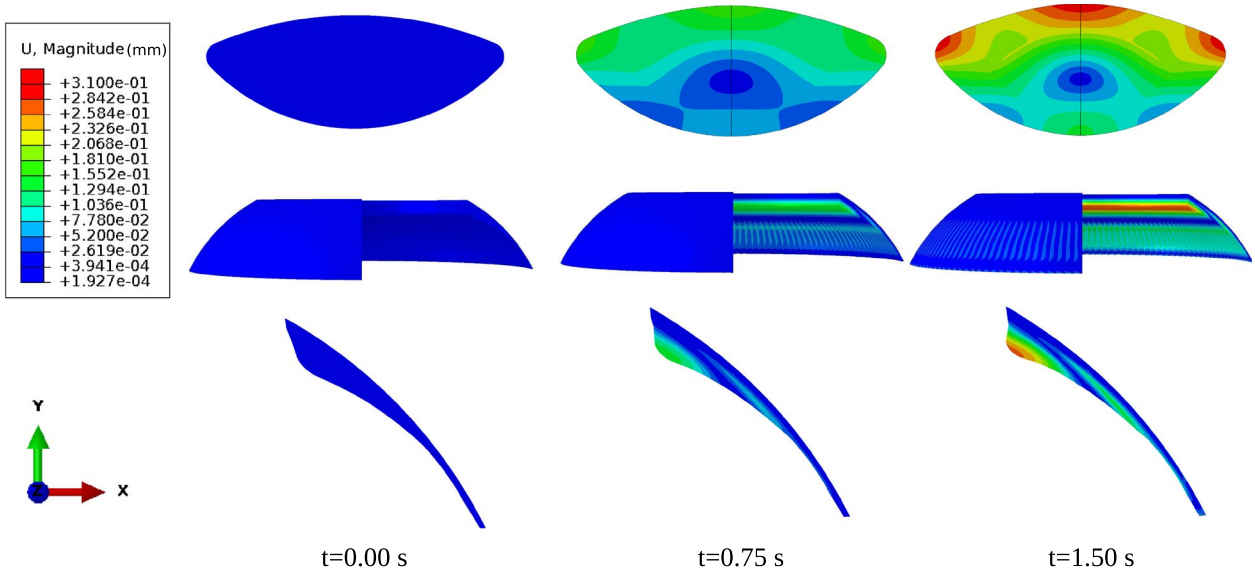

FIGURE 8 Morphological shape of the ciliary muscle and the lens in different moments of the accommodation process

and posterior lens radius of curvature against the actual accommodative change of the eye. This graph shows where the optical change is happening. Both surface curvatures fit perfectly according to the experimental data. However, the anterior radius of curvature does not fit as well at the end of accommodation. This result may be due to a slight inconsistency in the definition of the initial stresses of the lens capsule compared with the physiological values.

Figure 9b shows the changes in lens thickness (ΔT_L) and *ACD* as a function of the accommodative change. There is a ΔT_L of 0.44 mm and ΔACD of 0.31 mm for an accommodative change of 5.82 D. The orange line shows the change in the numerical nucleus thickness, which influences approximately 80% of the lens thickness, as previously reported.[7,31]

As a consequence of the increase in lens thickness, the lens moves anteriorly and posteriorly; see *Figure 9c*. The anterior lens movement is notably higher, approaching 0.31 mm anteriorly and 0.13 mm posteriorly for an accommodative change of 5.82 D.

Lens diameter (see *Figure 9d*) was compared with *ex vivo* experimental tests due to the difficulty of measuring the lens diameter *in vivo*. Data for a 29-year-old individual were obtained by interpolation from human groups aged 14 to 39.5 years as reported by Manns *et al*.[53] The numerical data fit perfectly with the interpolated data for a 29-year-old. All optical and biometric eye measurements were within the deviation reported by Ramasubramanian and Glasser.[18,19]

Analysing the influence of lens mechanical properties in presbyopia

The mechanical properties of the lens are fundamentally related to how it changes its shape,[8,10,26] above other factors such as the lens geometry.[15] Therefore, we analysed the decrease in accommodation amplitude by varying the mechanical properties, i.e., the lens capsule, nucleus and cortex, while we kept the remaining tissues of the FE model proposed for the 29-year-old subject constant. Thus, in this

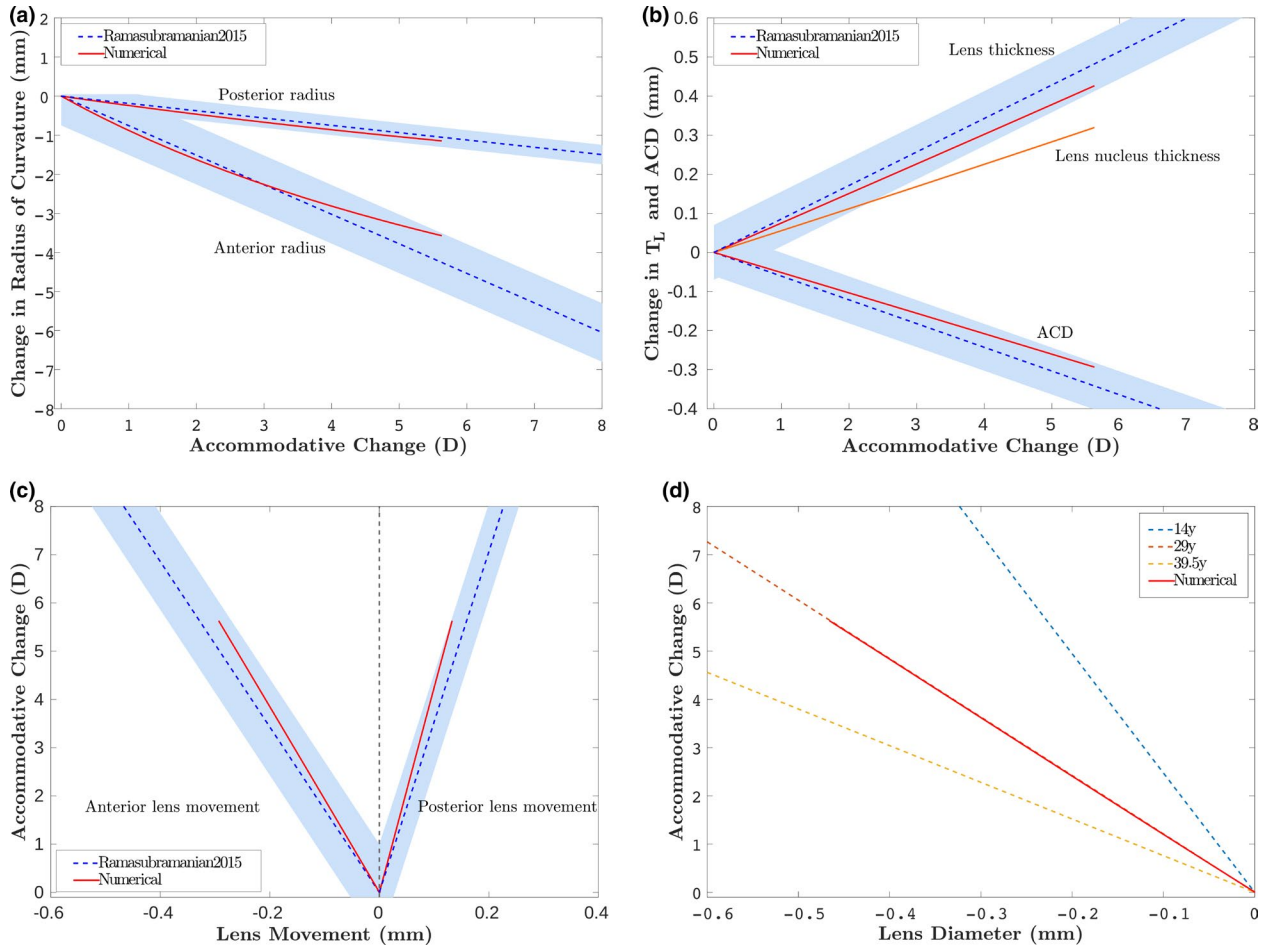

FIGURE 9 (a) Change in the anterior (r_a) and posterior (r_p) lens radius of curvature, (b) lens thickness (T_L) and anterior chamber distance (*ACD*), (c) anterior and posterior lens movement and (d) lens diameter, as functions of the change in accommodation

hypothetical case, we kept the same lens geometry and the initial stresses of the lens capsule calculated for the validated FE model, as reflected in *Figure 4a*.

We analysed three different cases: Case A, corresponding to all mechanical properties being fixed for a 29-year-old subject, except for the mechanical properties of the lens nucleus and cortex; Case B is the same as A, but with the change in the anterior and posterior lens capsule and Case C is a combination of Cases A and B. Both the mechanical properties of the lens capsule, nucleus and cortex were modified according to aging experimental data,[25,26] see *Figure 3b*.

Figure 10 shows the accommodation amplitude data as a function of age for three different numerical cases against the experimental data.[21-23] Case B, changing the mechanical properties of the lens capsule, presents a small decrease in accommodation amplitude, from 5.82 D for a 29-year-old subject to 4.24 D for a 51-year-old. By contrast, Cases A and C, where the mechanical properties of the lens nucleus and cortex change with age, present decreasing amplitudes similar to the experimental data.[21-23]

DISCUSSION

The main goal of this study was to develop an FE model that reproduced the *in vivo* accommodation process in humans. The proposed model reproduced Helmholtz's theory of accommodation and compared successfully with quality experimental data.[18-20] We accomplished this goal by quantifying contraction of the ciliary muscle and the optical and biometric measurements of accommodation, see *Figures 6* and *9*.

The resulting movement of the ciliary muscle comes from simultaneous contraction of the circular, radial and longitudinal muscle fibres. We faithfully reproduced the morphological changes in the ciliary muscle contraction of an emmetropic eye[20] by means of a computational eye model, which includes continuum and structural mechanics.[16,17] The morphological changes in the numerical and experimental ciliary muscle were similar, contracting towards the lens equator to release the resting tension on the zonular fibres, see *Figure 6*. This action was produced mainly by the circular muscle fibres, which governed ciliary muscle contraction. The numerical ciliary muscle became

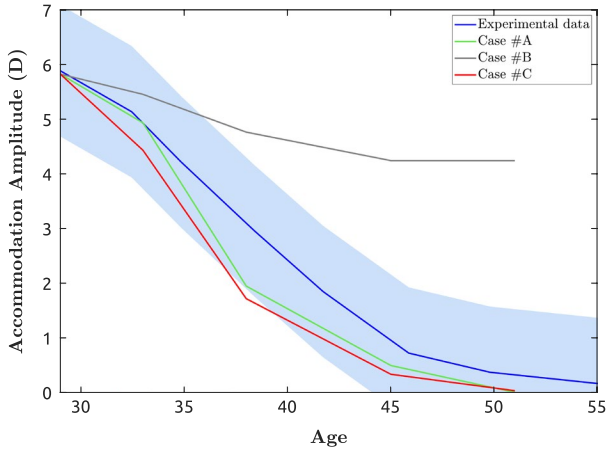

FIGURE 10 Decrease in accommodative amplitude with age. Experimental[21-23] and numerical data are compared

slightly thinner below the apex of the ciliary muscle, in contrast with the experimental values.[20] However, detecting small changes is highly difficult experimentally because the OCT measurement technique depends upon the patient's sclera radius of curvature and on the operator.[33]

The longitudinal muscle fibres appear to have little influence on ciliary muscle contraction. It is true that there is a slight decrease in the length of the ciliary muscle as a result of pulling the posterior part of the ciliary muscle forward to the scleral spur. However, the circular fibres contract slightly upwards intrinsically due to the geometry of the muscle itself, and not due to the contraction of the longitudinal fibres. This might be due to the boundary condition applied in the sclera, which made the interaction between the ciliary muscle and the sclera too stiff. On the other hand, Glasser reported[4] that the longitudinal fibres seem to brace the system rapidly so that the contraction of the inner portion is most effective; this is consistent with the numerical results obtained in the present study.

One weakness of the FE model is that we modelled the radial muscle fibres as a mixture of circular and longitudinal muscle fibres due to limitations in numerically designing the radial fibres. The radial muscle fibres are supposed to perform a combined effect of the circular and longitudinal fibres.[4] Another weakness is that the iris constriction, which increases the depth of focus of the eye, was not simulated because it is not relevant from a mechanical point of view.

Two of the limitations of the FE model arose from a lack of data in the literature. First, we considered that all muscular fibres were activated equally, although the force exerted, which depends on the force-stretch relationship (f_λ), was higher for the circular fibres. Second, the muscle properties were calibrated according to a virtual case based on the electrical innervation provided to rhesus monkeys by Glasser *et al*.[52] Nevertheless, the ciliary muscle could be updated according to new investigations with the proposed methodology.

The joint performance of the ciliary muscle and lens with respect to accommodation was analysed numerically. We obtained a linear response with an increase in accommodation of 5.82 D and an increase in T_L of 0.44 mm for a reduction of 0.66 mm in the ciliary muscle ring diameter ($\Delta\phi_{CM}$), or 67.54 μm in the maximum ciliary muscle thickness (ΔCMT_{max}). These values were within the range reported in the literature. Strenk *et al*.[54] reported $\Delta\phi_{CM}$ values ranging from 0.50 to 1.00 mm for an 8 D accommodative stimulus. Ruggeri *et al*.[55] reported ΔT_L and ΔCMT_{max} values of 0.20 mm and 72.0 μm, respectively, for an accommodation stimulus of 4 D in a 22-year-old subject. Additionally, Richdale *et al*.[51] reported a ΔT_L of 0.38 mm and ΔCMT_{max} of 98.41 μm for a 5.85 D accommodative response in a 29-year-old subject (taken from their fitted regression line). Although these values are within the range of the numerical values reported, it is difficult to compare the ΔCMT_{max} values because the experimental measurements depend upon the technique applied and the image quality.

Human accommodation is similar to that of other hominids. However, depending on the species and age, accommodation occurs in slightly different ways; for example, lens thickness and diameter change in humans is reduced compared with rhesus monkeys for the same accommodation amplitude.[3,19,53,56] For this reason, validating the main optical and biometric lens measurements was complicated and meaningful.

In this study, we present a numerical approach standardised for a 29-year-old individual, accurately reproducing human accommodation. The optical and biometric measurements of the lens were compared with *in vivo* accommodation dynamic measurements by Ramasubramanian and Glasser,[18,19] and all the numerical data presented were within the range of the experimental measurements. To achieve this aim, we previously reported that the mechanical properties of the crystalline lens are key to how the lens shape changes.[15] The presented model indicates that several factors such as lens mechanical properties, the zonular arrangement and capsule thickness distribution must be included to simulate the accommodation of humans.

We hypothesise that the stresses in the non-accommodated lens capsule should vary little over time for two reasons. Were they to increase, then accommodation would become higher over time while if they were to decrease, then the stiffness added with age would cause an earlier appearance of presbyopia. With this hypothesis, we determined that stiffening of the lens nucleus was mainly responsible for the decrease in accommodation amplitude (see *Figure 10*), rather than the increased stiffness in the lens capsule with increasing age. This conclusion is supported by our previous work,[15] where we observed that the stiffness ratio between the lens nucleus and cortex is key to how the lens changes its shape. In contrast to Wilkes *et al*.,[12] our FE model can explain some causes of presbyopia over a wider age range. Additional studies considering more factors involved in accommodation as well as mechanical data regarding the internal properties of the lens are needed to understand presbyopia further.

In contrast to other FE models that stretched the lens, simulating *ex vivo* conditions,[8-14] we designed our reference configuration using non-accommodated geometry. Designing the 3D FE model in this way allowed us to take lens movement into consideration, which is essential because changes in lens curvature do not reflect all significant accommodative changes.[57] In the numerical validation, 0.97 D (16%) of the 5.82 D of the accommodation amplitude was produced by lens movement. Furthermore, this model could be compared with novel research from the literature[18-20] and provides the necessary background to analyse and evaluate fundamental aspects of accommodation, as well as the detailed geometry of a 29-year-old individual for other research studies.

ACKNOWLEDGEMENTS

We would like to thank Adrian Glasser for the helpful and comprehensive discussions on this project. The authors also gratefully acknowledge research support from the Spanish Ministerio de Ciencia, Innovacion y Universidades (Grant DPI2017-84047-R) and the Department of Industry and Innovation (Government of Aragon) through the research group Grant T24-20R (cofinanciado con Feder 2014-2020: Construyendo Europa desde Aragon). Part of the work was performed by the ICTS "NANBIOSIS" specifically by the High Performance Computing Unit (U27), of the CIBER in Bioengineering, Biomaterials & Nanomedicne (CIBER-BBN at the University of Zaragoza). I. Cabeza-Gil was supported by PRE2018-084021.

CONFLICT OF INTEREST

The authors report no conflicts of interest and have no proprietary interest in any of the materials mentioned in this article.

AUTHOR CONTRIBUTIONS

Iulen Cabeza-Gil: Conceptualization (equal); Methodology (equal); Software (equal); Writing-original draft (equal). **Jorge Grasa:** Resources (equal); Software (equal); Supervision (equal); Writing-review & editing (equal). **Begoña Calvo:** Conceptualization (equal); Project administration (equal); Supervision (equal); Writing-review & editing (equal).

ORCID

Iulen Cabeza-Gil https://orcid.org/0000-0001-8219-2365

REFERENCES

1. Helmholtz H. Ueber die accommodation des auges. A*lbrecht von Graefes Arch Klin Expl Ophtalmol*. 1855;2:1–74.
2. Fincham F. The changes in the form of the crystalline lens in accommodation. *Trans Opt Soc*. 1925;26:239–269.
3. Glasser A, Kaufman PL. The mechanism of accommodation in primates. *Ophthalmology*. 1999;106:863–872.
4. Levin LA, Nilsson SFE, Ver Hoeve J, Wu S, Kaufman PL, Alm A (Eds.). Adler's Physiology of the Eye. Chapter 3 (A. Glasser): Accommodation. Edingburg: Elsevier Health Sciences; 2011.
5. Tamm S, Tamm E, Rohen JW. Age-related changes of the human ciliary muscle. A quantitative morphometric study. *Mech Ageing Dev*. 1992;62:209–221.
6. Pardue MT, Sivak JG. Age-related changes in human ciliary muscle. *Optom Vis Sci*. 2000;77:204–210.
7. Brown N. The change in shape and internal form of the lens of the eye on accommodation. *Exp Eye Res*. 1973;15:441–459.
8. Burd HJ, Judge SJ, Cross JA. Numerical modelling of the accommodating lens. *Vis Res*. 2002;42:2235–2251.
9. Hermans EA, Dubbelman M, van der Heijde GL, Heethaar RM. Estimating the external force acting on the human eye lens during accommodation by finite element modelling. *Vis Res*. 2006;46:3642–3650.
10. Van de Sompel D, Kunkel GJ, Hersh PS, Smits AJ. Model of accommodation: contributions of lens geometry and mechanical properties to the development of presbyopia. *J Cataract Refract Surg*. 2010;36:1960–1971.
11. Lanchares E, Navarro R, Calvo B. Hyperelastic modelling of the crystalline lens: accommodation and presbyopia. *J Optom*. 2012;5:110–120.
12. Wilkes RP, Reilly MA. A pre-tensioned finite element model of ocular accommodation and presbyopia. *Int J Adv Eng Sci Appl Math*. 2015;8:25–38.
13. Wang K, Venetsanos D, Wang J, Pierscionek BK. Gradient moduli lens models: how material properties and application of forces can affect deformation and distributions of stress. *Sci Rep*. 2016;6:31171. https://doi.org/10.1038/srep31171
14. Wang K, Venetsanos DT, Hoshino M, Uesugi K, Yagi N, Pierscionek BK. A modeling approach for investigating opto-mechanical relationships in the human eye lens. *IEEE Trans Biomed Eng*. 2020;67:999–1006.
15. Cabeza-Gil I, Grasa J, Calvo B. A numerical investigation of changes in lens shape during accommodation. *Sci Rep*. 2021;11:9639. https://doi.org/10.1038/s41598-021-89145-z
16. Hernández-Gascón B, Grasa J, Calvo B, Rodríguez JF. A 3D electromechanical continuum model for simulating skeletal muscle contraction. *J Theor Biol*. 2013;335:108–118.
17. Grasa J, Sierra M, Lauzeral N, Muñoz MJ, Miana-Mena FJ, Calvo B. Active behavior of abdominal wall muscles: experimental results and numerical model formulation. *J Mech Behav Biomed Mater*. 2016;61:444–454.
18. Ramasubramanian V, Glasser A. Can ultrasound biomicroscopy be used to predict accommodation accurately? *J Refract Surg*. 2015;31:266–273.
19. Ramasubramanian V, Glasser A. Objective measurement of accommodative biometric changes using ultrasound biomicroscopy. *J Cataract Refract Surg*. 2015;41:511–526.
20. Wagner S, Zrenner E, Straßer T. Emmetropes and myopes differ little in their accommodation dynamics but strongly in their ciliary muscle morphology. *Vis Res*. 2019;163:42–51.
21. Koretz JF, Kaufman PL, Neider MW, Goeckner PA. Accommodation and presbyopia in the human eye-aging of the anterior segment. *Vis Res*. 1989;29:1685–1692.
22. Ostrin LA, Glasser A. Accommodation measurements in a pre-presbyopic and presbyopic population. *J Cataract Refract Surg*. 2010;36:1960–71.
23. Anderson HA, Hentz G, Glasser A, Stuebing KK, Manny RE. Minus-lens–stimulated accommodative amplitude decreases sigmoidally with age: a study of objectively measured accommodative amplitudes from age 3. *Invest Ophthalmol Vis Sci*. 2008;49:2919–2926.
24. Fisher RF. Elastic constants of the human lens capsule. *J Physiol*. 1969;201:1–19.
25. Weeber HA, Eckert G, Pechhold W, Heijde RGL. Stiffness gradient in the crystalline lens. *Graefes Arch Clin Exp Ophthalmol*. 2007;245:1357–1366.
26. Wilde GS, Burd HJ, Judge SJ. Shear modulus data for the human lens determined from a spinning lens test. *Exp Eye Res*. 2012;97:36–48.
27. Chang Y-C, Mesquita GM, Williams S, *et al*. In vivo measurement of the human crystalline lens equivalent refractive index using extended- depth OCT. *Biomed Opt Express*. 2019;10:411–422.
28. Barraquer RI, Michael R, Abreu R, Lamarca J, Tresserra F. Human lens capsule thickness as a function of age and location along the sagittal lens perimeter. *Invest Ophthalmol Vis Sci*. 2006;47:2053–2060.

29. Kasthurirangan S, Markwell EL, Atchison DA, Pope JM. MRI study of the changes in crystalline lens shape with accommodation and aging in humans. *J Vis*. 2011;11:19,1–16.
30. Dubbelman M, Heijde GL, Van WHA, Vrensen GFJM. Changes in the internal structure of the human crystalline lens with age and accommodation. *Vis Res*. 2003;43:2363–2375.
31. Hermans E, Dubbelman M, Heijde R, Heethaar R. The shape of the human lens nucleus with accommodation. *J Vis*. 2007;7:16. https://doi.org/10.1167/7.10.16
32. Bernal A, Jean-Marie P, Manns F. Evidence for posterior zonular fiber attachment on the anterior hyaloid membrane. *Invest Ophthalmol Vis Sci*. 2006;47:4708–4713.
33. Straßer T, Wagner S, Zrenner E. Review of the application of the open-source software CilOCT for semi-automatic segmentation and analysis of the ciliary muscle in OCT images. *PLoS One*. 2020;15:e0234330.
34. Lee RY, Huang G, Porco TC, Chen Y, He M, Lin SC. Differences in iris thickness among African Americans, Caucasian Americans, Hispanic Americans, Chinese Americans, and Filipino-Americans. *J Glaucoma*. 2013;22:673–678.
35. Fernández-Vigo JI, García-Feijóo J, Martínez-de-la-Casa JM, *et al*. Fourier domain optical coherence tomography to assess the iridocorneal angle and correlation study in a large Caucasian population. *BMC Ophthalmol*. 2016;16:42. https://doi.org/10.1186/s12886-016-0219-z
36. Le-Grand Y, El-Hage SG. Physiological Optics. (Translation and update of Le Grand Y, La dioptrique de l'oeil et sa correction), vol. 1. Heidelberg: Springer-Verlag. 1968; p. 57–69.
37. Siu A, Herse P. The effect of age on human corneal thickness. *Acta Ophthalmol*. 2009;71:51–56.
38. Stålhand J, Klarbring A, Holzapfel GA. A mechanochemical 3D continuum model for smooth muscle contraction under finite strains. *J Theor Biol*. 2011;268:120–130.
39. Mallen EA, Gilmartin B, Wolffsohn JS. Sympathetic innervation of ciliary muscle and oculomotor function in emmetropic and myopic young adults. *Vis Res*. 2005;45:1641–1651.
40. Calvo B, Sierra M, Grasa J, Muñoz MJ, Peña E. Determination of passive viscoelastic response of the abdominal muscle and related constitutive modeling: stress-relaxation behavior. *J Mech Behav Biomed Mater*. 2014;36:47–58.
41. Krag S, Andreassen TT. Mechanical properties of the human lens capsule. *Prog Retin Eye Res*. 2003;22:749–767.
42. Krag S, Andreassen TT. Mechanical properties of the human posterior lens capsule. *Invest Ophthalmol Vis Sci*. 2003;44:691–696.
43. Burd HJ, Wilde GS, Judge SJ. Can reliable values of Young's modulus be deduced from Fisher's (1971) spinning lens measurements? *Vis Res*. 2006;46:1346–1360.
44. Heys KR, Cram SL, Truscott RJW. Massive increase in the stiffness of the human lens nucleus with age: the basis for presbyopia? *Mol Vis*. 2004;10:956–963.
45. Michael R, Mikielewicz M, Gordillo C, *et al*. Elastic properties of human lens zonules as a function of age in presbyopes. *Invest Ophthalmol Vis Sci*. 2012;53:6109–6114.
46. Friberg TR, Lace JW. A comparison of the elastic properties of human choroid and sclera. *Exp Eye Res*. 1988;47:429–436.
47. Li C, Guan G, Huang Z, Johnstone M, Wang RK. Noncontact all-optical measurement of corneal elasticity. *Opt Lett*. 2012;37:1625. https://doi.org/10.1364/OL.37.001625
48. Alphen G, Graebel WP. Elasticity of tissues involved in accommodation. *Vis Res*. 1991;31:1417–1438.
49. Glasser A, Campbell MCW. Biometric, optical and physical changes in the isolated human crystalline lens with age in relation to presbyopia. *Vis Res*. 1999;39:1991–2015.
50. Schmid KL, Strang NC. Differences in the accommodation stimulus response curves of adult myopes and emmetropes: a summary and update. *Ophthalmic Physiol Opt*. 2015;35:613–621.
51. Richdale K, Sinnott LT, Bullimore MA, *et al*. Quantification of age-related and per diopter accommodative changes of the lens and ciliary muscle in the emmetropic human eye. *Invest Ophthalmol Vis Sci*. 2013;54:1095–1105.
52. Glasser A, Wendt M, Ostrin L. Accommodative changes in lens diameter in rhesus monkeys. *Investig Ophthalmol Vis Sci*. 2006;47:ARVO E-Abstract 278.
53. Manns F, Parel J-M, Denham D, *et al*. Optomechanical response of human and monkey lenses in a lens stretcher. *Invest Ophthalmol Vis Sci*. 2007;48:3260–3268.
54. Strenk SA, Semmlow JL, Strenk LM, *et al*. Age-related changes in human ciliary muscle and lens: a magnetic resonance imaging study. *Invest Ophthalmol Vis Sci*. 1999;40:1162–1169.
55. Ruggeri M, de Freitas C, Williams S, *et al*. Quantification of the ciliary muscle and crystalline lens interaction during accommodation with synchronous OCT imaging. *Biomed Opt Express*. 2016;7:1351–1364.
56. Vilupuru AS, Glasser A. The relationship between refractive and biometric changes during Edinger-Westphal stimulated accommodation in rhesus monkeys. *Exp Eye Res*. 2005;80:349–360.
57. Croft MA, Heatley G, McDonald JP, Katz A, Kaufman PL. Accommodative movements of the lens/capsule and the strand that extends between the posterior vitreous zonule insertion zone and the lens equator, in relation to the vitreous face and aging. *Ophthalmic Physiol Opt*. 2015;36:21–32.

How to cite this article: Cabeza-Gil I, Grasa J, Calvo B. A validated finite element model to reproduce Helmholtz's theory of accommodation: a powerful tool to investigate presbyopia. *Ophthalmic Physiol Opt*. 2021;41:1241–1253. https://doi.org/10.1111/opo.12876